ChemComm

COMMUNICATION

View Article Online
View Journal | View Issue

Cite this: *Chem. Commun.*, 2016, 52, 10763

Received 5th July 2016,
Accepted 3rd August 2016

DOI: 10.1039/c6cc05550h

www.rsc.org/chemcomm

A crystalline anionic complex of scandium nitride endometallofullerene: experimental observation of single-bonded $(Sc_3N@I_h\text{-}C_{80}^-)_2$ dimers†

Dmitri V. Konarev,*[a] Leokadiya V. Zorina,[b] Salavat S. Khasanov,[b] Alexey A. Popov,[c] Akihiro Otsuka,[d] Hideki Yamochi,[d] Gunzi Saito[ef] and Rimma N. Lyubovskaya[a]

Reduction of scandium nitride clusterfullerene, $Sc_3N@I_h\text{-}C_{80}$, by sodium fluorenone ketyl in the presence of cryptand[2,2,2] allows the crystallization of the $\{cryptand[2,2,2](Na^+)\}_2(Sc_3N@I_h\text{-}C_{80}^-)_2\cdot 2.5C_6H_4Cl_2$ (1) salt. The $Sc_3N@I_h\text{-}C_{80}^{\bullet -}$ radical anions are dimerized to form single-bonded $(Sc_3N@I_h\text{-}C_{80}^-)_2$ dimers.

Endohedral metallofullerenes (EMFs) containing metal atoms inside fullerene cages have evoked great interest in many fields of research.[1] Numerous reports on the generation of EMF anions in solution and their spectroscopic characterization by NMR and EPR spectroscopies exist. Paramagnetic EMFs such as $M@C_{82}$ (M = La, Y) or $Sc_3C_2@C_{80}$ form stable diamagnetic anions;[2] the formation of solids based on these anions has been reported but without structural analysis.[3] Dimetallofullerenes and most clusterfullerenes (such as nitride clusterfullerene (NCF), *e.g.*, $Sc_3N@C_{80}$, studied in this work) are diamagnetic in the pristine state and form radical anions upon single-electron reduction. Several radical anions have been characterized by EPR spectroscopy in solution, including those of $Sc_3N@C_{80}$[4] and its derivatives.[5] However, the formation of "salts" based on clusterfullerene anions as well as single-crystal X-ray diffraction analyses has never been achieved. This is in sharp contrast to empty fullerenes, especially C_{60} and C_{70}, for which many anionic phases with various magnetic and conducting properties have been reported.[6,7]

The structural information on the radical anions of clusterfullerenes is important to understand the irreversible reduction behavior exhibited by many clusterfullerenes at moderate voltammetric scan rates.[8,9] A typical example of such reduction behavior is shown by the clusterfullerene $Sc_3N@C_{80}$: electrochemical reversibility of its reduction is achieved at relatively high scan rates (exceeding 5 V s^{-1}), whereas at low scan rates, a follow-up chemical reaction is involved.[9] Although the reduction of NCFs is electrochemically irreversible, it is chemically reversible and the nature of the follow-up process has not yet been fully disclosed. Possible dimerization of NCF anions was proposed based on EPR spectroscopy of the reduction products of $Sc_3N@C_{68}$ because the estimated spin number was an order of magnitude lower than that of the analogous cationic species.[10] Theoretical calculations also support the ability of NCF anions to dimerize not only in the solid state but also in solution,[11] whereas dimerization of the radical anions of empty fullerenes ($C_{60}^{\bullet -}$ and $C_{70}^{\bullet -}$) is observed in the solid state only.[7,12]

In this work, we obtained the first anionic complex of triscandium nitride clusterfullerene as single crystals of the $\{cryptand[2,2,2](Na^+)\}_2(Sc_3N@I_h\text{-}C_{80}^-)_2\cdot 2.5C_6H_4Cl_2$ composition (**1**) (henceforth, cryptand[2,2,2] is abbreviated to cryptand). Moreover, analysis of the crystal structure of **1** at 95 K reveals that the $Sc_3N@I_h\text{-}C_{80}^{\bullet -}$ radical anions dimerize to form single-bonded $(Sc_3N@I_h\text{-}C_{80}^-)_2$ dimers, indicating that anionic NCFs have a strong tendency to dimerize, similar to the radical anions of empty fullerenes.[7,12]

To prepare crystals of **1**, 10 mg of $Sc_3N@I_h\text{-}C_{80}$ was reduced in 10 ml of *o*-dichlorobenzene by excess sodium fluorenone ketyl (3 mg) in the presence of an equimolar amount of cryptand (4,7,13,16,21,24-hexaoxa-1,10-diazabicyclo[8.8.8]-hexacosane, 3.4 mg) to produce a brown solution. Slow mixing of this solution with *n*-hexane over 2 months produced small black blocks of **1** in 18% yield; their composition was determined by single crystal X-ray diffraction. Testing of several crystals obtained from the synthesis showed that only one crystal phase is formed. We found that different cations and NCFs can potentially be used to obtain crystalline salts. However, in some cases, insoluble

[a] *Institute of Problems of Chemical Physics RAS, Chernogolovka, Moscow region, 142432 Russia. E-mail: konarev3@yandex.ru*
[b] *Institute of Solid State Physics RAS, Chernogolovka, Moscow region, 142432 Russia*
[c] *Leibniz Institute for Solid State and Materials Research Helmholtzstraße 20, 01069 Dresden, Germany*
[d] *Division of Chemistry, Graduate School of Science, Kyoto University, Sakyo-ku, Kyoto 606-8502, Japan*
[e] *Faculty of Agriculture, Meijo University, 1-501 Shiogamaguchi, Tempaku-ku, Nagoya 468-8502, Japan*
[f] *Toyota Physical and Chemical Research Institute, 41-1, Yokomichi, Nagakute, Aichi 480-1192, Japan*

† Electronic supplementary information (ESI) available. CCDC 1487746. For ESI and crystallographic data in CIF or other electronic format see DOI: 10.1039/c6cc05550h

precipitates are formed quantitatively within minutes, as in the case of bis(triphenylphosphoranylidene)ammonium cations (PPN^+), which are insoluble even in polar benzonitrile. One possible reason for this behavior is polymerization of the NCF radical anions.

The structure of **1** was determined from a crystal that was slowly cooled to 95 K.‡ It contains a single-bonded $(Sc_3N@I_h\text{-}C_{80}^-)_2$ dimer, two cryptand(Na^+) cations and solvent $C_6H_4Cl_2$ molecules. Despite slow cooling, all components in the salt are strongly disordered. The $(Sc_3N@I_h\text{-}C_{80}^-)_2$ dimers are disordered between three orientations, with 0.441(3), 0.366(3), and 0.192(3) occupancies. Nevertheless, the geometry of the I_h-C_{80} cage and the Sc_3N fragment inside the cage as well as the presence of the intercage C–C bond between fullerenes are well established. There are four examples of structurally characterized EMF dimers: Li@C_{60},[13] the Bingel–Hirsch bisadduct of La@C_{82},[14] a mixed triazine/benzyl derivative of $La_2@I_h$-C_{80},[15] and Y@C_s(6)-C_{82},[16] which are reported to dimerize spontaneously to form single-bonded dimers. In all these cases, the dimers are neutral and have radical EMFs as precursors.

The fullerene C_{80} cage has symmetry close to I_h in **1**. Theoretical calculations showed that the $Sc_3N@I_h\text{-}C_{80}^-$ anions can dimerize to form the intercage C–C bond by carbon atoms on the pentagon–hexagon–hexagon junction (PHHJ) as well as on the hexagon–hexagon–hexagon junction (THJ). The PHHJ dimer is approximately 8 kJ mol^{-1} more stable than the THJ dimer.[11] The $Sc_3N@I_h\text{-}C_{80}^-$ anions have *trans*-orientation in the dimers of **1**. Indeed, both types of dimers are found. The THJ dimer has 0.441(3) occupancy (Fig. 1a and b), and the PHHJ dimer has 0.366(3) (Fig. 1c and d) and 0.192(3) occupancies. Therefore, the disorder of the dimers is intrinsic and can be explained by the crystallization of both types of dimers in the crystal. The "mixed" asymmetric PHHJ–THJ dimers have a mean relative energy that falls between those characteristic of the corresponding symmetric dimers[11] and potentially can also form in **1**. However, X-ray diffraction analysis does not allow distinguishing such dimers in the mixture of the symmetric PHHJ and THJ dimers. Fig. 1 shows that the Sc_3N clusters have very similar orientations with respect to the intercage bonding sites in both dimers. In addition to the dimer of $La_2@C_{80}$, single-bonded derivatives of EMFs with I_h-C_{80} cages have been reported recently; the benzyl adduct of $La_2@C_{80}$ is formed *via* a PHHJ carbon,[17] the carbene adduct to $Sc_3N@C_{80}$ is formed *via* a THJ carbon[18] (note that the orientation of the Sc_3N cluster inside the cage in the carbene adduct is very similar to that in the dimer reported in this work), and the Bingel addition to $TiY_2N@C_{80}$ occurs at the PHHJ site.[19] Recently, a single-bonded neutral PHHJ $\{Y@C_s(6)\text{-}C_{82}\}_2$ dimer was found.[16] In all cases, single isomers were formed selectively. However, computation shows that the PHHJ and THJ single-bonded adducts are virtually isoenergetic for EMFs with the C_{80}-I_h cage. The formation of both PHHJ and THJ dimers in this work may indicate an equilibrium distribution of dimer isomers. The possible observation of reversible reduction at high scan rates as well as EPR-detectable radical anions in solution[4,9] shows that the $(Sc_3N@C_{80}^-)_2$ dimer is probably in dynamic equilibrium with monomeric $Sc_3N@C_{80}^{\bullet -}$ anion radicals. The presence of this equilibrium would also explain the co-crystallization of THJ and PHHJ dimers with some prevalence of the more thermodynamically stable PHHJ dimer. It is known that the $(C_{60}^-)_2$ and $(C_{70}^-)_2$ dimers are formed only through PHHJ carbon atoms.[7,12]

The geometry of the starting material, $Sc_3N@I_h$-C_{80}, was studied in the molecular complex $Co^{II}OEP{\cdot}Sc_3N@I_h\text{-}C_{80}{\cdot}0.5C_6H_6{\cdot}1.5CHCl_3$ (OEP: octaethylporphyrin).[20] $Sc_3N@I_h$-C_{80} molecules are nearly spherical in the neutral state. The average distances between the midpoints of the three oppositely located 6–6 C–C bonds in three orthogonal directions are 8.136, 8.136, and 8.203 Å. The Sc_3N fragment in $Sc_3N@I_h$-C_{80} is rather symmetric, with two shorter Sc–N bonds 1.966(12) Å in length and one longer Sc–N bond 2.011(19) Å in length (the average length is 1.981(14) Å). At the same time, the Sc–N–Sc angles are close to each other, being 115.5(11), 122.2(6), and 122.2(6)°. Scandium atoms form short Sc–C contacts with the carbon atoms of the cage (2.15(1) to 2.19(1) Å in length).[20]

The formation of intercage C–C bonds between two $Sc_3N@I_h\text{-}C_{80}^-$ anions in most occupied orientations of the THJ dimer results in a strong deviation of the C_{80} cage from I_h symmetry, accompanied by elongation of the cage along the long axis of the dimer. As a result, the distances between the midpoints of the three oppositely located 6–6 C–C bonds in three orthogonal directions for the $Sc_3N@I_h\text{-}C_{80}^-$ sphere in **1** are 8.134, 8.203, and 8.293 (long axis) Å. This elongation affects the geometry of the Sc_3N fragments inside the cage. The Sc–N bonds are equalized to be 2.034(6), 2.052(6), and 2.062(6) Å, and the average length of these bonds is 2.050(6) Å. At the same time, the Sc–N–Sc angles vary due to the elongation of the cage (96.4(3), 131.1(3), and 132.2(4)°), whereas these angles are close to 120° in pristine $Sc_3N@I_h$-C_{80}.[20]

The length of a single intercage C–C bond in $(Sc_3N@I_h\text{-}C_{80}^-)_2$ is equal to 1.642(14) Å for the PHHJ dimer and 1.636(14) Å for

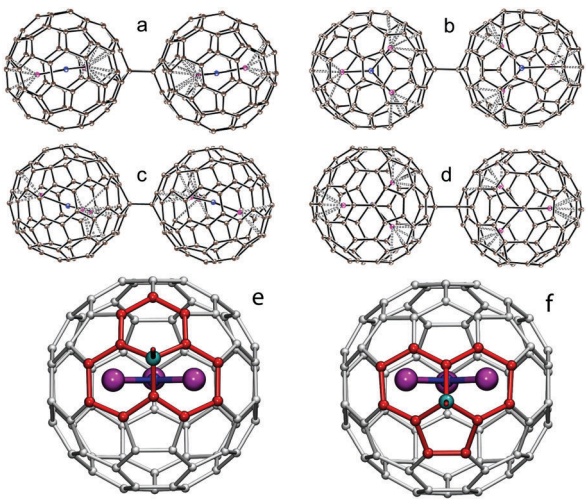

Fig. 1 Molecular structures of the THJ $(Sc_3N@I_h\text{-}C_{80}^-)_2$ dimer with 0.441(3) occupancy along (a) and approximately on (b) the Sc_3N plane; the PHHJ $(Sc_3N@I_h\text{-}C_{80}^-)_2$ dimer with 0.366(3) occupancy along (c) and approximately on (d) the Sc_3N plane. Short Sc···C(C_{80}) contacts inside the cages are shown by dashed lines. Fragments of the THJ (e) and PHHJ (f) dimers that participated in the formation of intercage C–C bonds.

the THJ dimer. These are the longest intercage C–C bonds among single-bonded fullerene dimers; however, the accuracy of the determination of the length of these bonds is low. The $(C_{60}^-)_2$ and $(C_{70}^-)_2$ dimers have intercage C–C bonds 1.587(4) to 1.597(7) and 1.583(2) to 1.586(3) Å in length,[7,12] respectively. Three scandium atoms positioned inside the I_h-C_{80} cage form multiple Sc···C(C_{80}) contacts whose lengths are in the 2.052(13) to 2.477(13) Å range (shown by dashed lines in Fig. 1).

The driving force for the dimerization is not yet clear. Presumably it lies in the spin-density distribution in $Sc_3N@I_h$-$C_{80}^{\bullet -}$. In contrast to empty fullerenes, whose spin density is uniformly delocalized over the cage, in the NCF anion the spin density is localized on the cluster and on few cage atoms.[21] In particular, on three PHHJ carbons whose positions with respect to the Sc atoms are similar to those in the dimer.

Salt **1** has a layered structure in which endometallofullerene layers alternate with organic layers composed of the cryptand(Na^+) cations and $C_6H_4Cl_2$ molecules along the *a* axis. Both layers are penetrated by continuous chains from the $C_6H_4Cl_2$ molecules arranged along the *a* axis. The $Sc_3N@I_h$-C_{80}^- anions in the layers have strongly distorted hexagonal arrangements, with six neighbors for each anion (Fig. 2a). One fullerene neighbor originates from the same dimer; however, the other neighbors belong to four different dimers. Short van der Waals contacts are formed for four of the five fullerene neighbors. In the presence of spins on EMF anions, this packing can provide promising magnetic and/or conducting properties. This situation can occur when the dimers dissociate (similarly to the $(C_{60}^-)_2$ and $(C_{70}^-)_2$ dimers[7,12]), forming radical anions at high temperature.

Pristine $Sc_3N@I_h$-C_{80} does not have noticeable absorption in the NIR range (Fig. 3). The formation of $Sc_3N@I_h$-C_{80}^- anions and their dimerization causes two poorly resolved bands to appear in the NIR range at approximately 870 and 990 nm (Fig. 3). The appearance of two bands is characteristic of negatively charged fullerene dimers. For example, single-bonded $(C_{70}^-)_2$ dimers also show two NIR bands at 880 and 1240 nm.[7,12] The PBE/TZ2P-predicted HOMO–LUMO gaps are 1.157 eV for THJ dimers and 1.098 eV for PHHJ dimers (for pristine $Sc_3N@C_{80}$, the theoretically predicted gap is 1.463 eV). TD-DFT calculations predict moderate intensity transitions across the bandgap with energies close to the HOMO–LUMO gap. These transitions presumably correspond to the NIR absorption bands at 990 nm in the experimental spectrum. The HOMOs of both dimers are partially localized on the Sc atoms and partially on an intercage C–C bond, whereas the LUMOs are more delocalized between the Sc_3N cluster and the C_{80} cages (Fig. 3 and Fig. S5, ESI†).

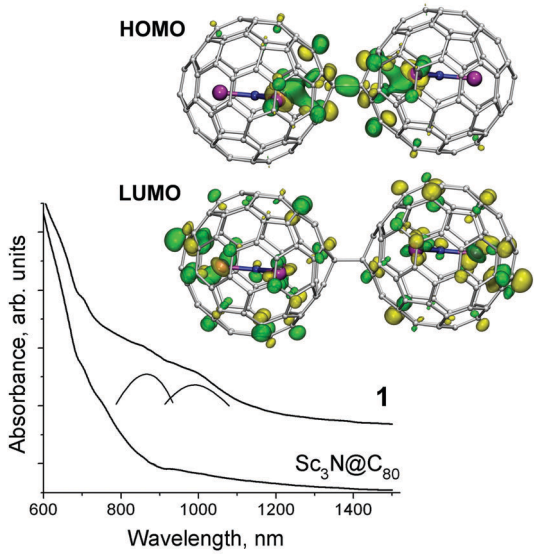

Fig. 3 HOMO and LUMO isosurfaces of the PHHJ dimer; visible-NIR spectrum of the starting material $Sc_3N@I_h$-C_{80} and salt **1** in KBr pellets prepared under anaerobic conditions. The position of the bands in the spectrum of **1** is shown by arcs.

IR spectra of $Sc_3N@I_h$-C_{80} and salt **1** are shown in the ESI† (Table S1 and Fig. S1). The main IR absorption bands of $Sc_3N@I_h$-C_{80} are reproduced in the spectrum of **1**. An intense split band at 1381 and 1370 cm^{-1} appears in the spectrum of **1** nearly at the same position. An intense band at 600 cm^{-1}

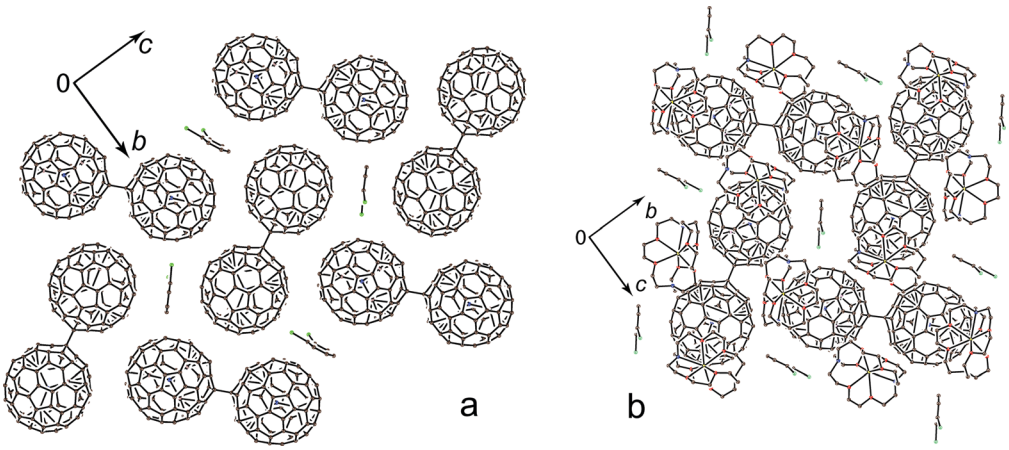

Fig. 2 (a) Layers composed of $(Sc_3N@I_h$-$C_{80}^-)_2$ dimers and $C_6H_4Cl_2$ molecules arranged in the *bc* plane and (b) projection of the organic layer composed of cryptand(Na^+) cations and $C_6H_4Cl_2$ molecules on the endometallofullerene layer. Only major occupied orientations for all components are shown.

attributed to the antisymmetric Sc–N stretching ν_{as}(Sc–N) mode[22] is up-shifted and split into two main components at 645 and 658 cm^{-1} (Fig. S1, ESI†). According to computational studies, dimerization lifts the twofold degeneracy of this mode and causes up-shifting of its component with high IR intensity. Moreover, the frequencies of the ν_{as}(Sc–N) mode in the PHHJ and THJ dimers are different, which presumably results in the complex shape of the experimental band with two main peaks (Fig. S1, ESI†), supporting the observations of the THJ and PHHJ dimers in **1**. Another characteristic mode of the dimer is localized predominantly on the intercage bond; this corresponds to the medium-intensity absorption bands near 798 and 802 cm^{-1} (Fig. S1, ESI†).

In conclusion, the preparation of the first anionic complex of $Sc_3N@I_h$-C_{80} as a single crystal opens a new field of research associated with anion and radical anion complexes of EMFs, which was successfully developed for empty fullerenes.[6,7,23] These complexes can potentially combine promising magnetic and/or conducting properties. Moreover, the $Sc_3N@I_h$-$C_{80}^{\bullet-}$ radical anions as was theoretically predicted have a strong tendency to dimerize, forming single-bonded $(Sc_3N@I_h$-$C_{80}^{-})_2$ dimers. We believed that this tendency can result in dimeric and even polymeric anions of EMFs.

This work was supported by the Russian Science Foundation (project No. 14-13-00028) and by JSPS KAKENHI Grant numbers JP23225005 and JP26288035. AAP acknowledges funding by DFG (grant PO 1602/1-2) and the European Research Council (ERC) under the European Union's Horizon 2020 research and innovation program (grant agreement No. 648295 ''GraM3'').

Notes and references

‡ Crystal data for **1**: $C_{211}H_{82}Cl_5N_6Na_2O_{12}Sc_6$, F.W. 3385.81, black prism, 0.220 × 0.110 × 0.006 mm^3; 95(2) K; monoclinic, space group $P2_1/c$, a = 15.1344(9) Å, b = 20.6079(13) Å, c = 21.8351(12) Å, β = 90.019(6)°, V = 6810.1(7) $Å^3$, Z = 2, d_{calcd} = 1.651 M gm^{-3}, μ = 0.469 mm^{-1}, $F(000)$ = 3438, $2\theta_{max}$ = 48.262°; 50 523 reflections collected, 10 825 independent; R_1 = 0.1401 for 5385 observed data [$I > 2\sigma(F)$] with 35 972 restraints and 1935 parameters; wR_2 = 0.3943 (all data); final G.o.F. = 1.319. CCDC 1487746.

1 A. A. Popov, S. Yang and L. Dunsch, *Chem. Rev.*, 2013, **113**, 5989–6113; R. B. Ross, C. M. Cardona, D. M. Guldi, S. G. Sankaranarayanan, M. O. Reese, N. Kopidakis, J. Peet, B. Walker, G. C. Bazan, E. Van Keuren, B. C. Holloway and M. Drees, *Nat. Mater.*, 2009, **8**, 208–212; H. Kato, Y. Kanazawa, M. Okumura, A. Taninaka, T. Yokawa and H. Shinohara, *J. Am. Chem. Soc.*, 2003, **125**, 4391–4397.
2 T. Tsuchiya, T. Wakahara, Y. Maeda, T. Akasaka, M. Waelchli, T. Kato, H. Okubo, N. Mizorogi, K. Kobayashi and S. Nagase, *Angew. Chem., Int. Ed.*, 2005, **44**, 3282–3285; Y. Iiduka, T. Wakahara, T. Nakahodo, T. Tsuchiya, A. Sakuraba, Y. Maeda, T. Akasaka, K. Yoza, E. Horn, T. Kato, M. T. H. Liu, N. Mizorogi, K. Kobayashi and S. Nagase, *J. Am. Chem. Soc.*, 2005, **127**, 12500–12501; L. Feng, T. Wakahara, T. Tsuchiya, Y. Maeda, Y. F. Lian, T. Akasaka, N. Mizorogi, K. Kobayashi, S. Nagase and K. M. Kadish, *Chem. Phys. Lett.*, 2005, **405**, 274–277.
3 I. E. Kareev, E. Laukhina, V. P. Bubnov, V. M. Martynenko, V. Lloveras, J. Vidal-Gancedo, M. Mas-Torrent, J. Veciana and C. Rovira, *ChemPhysChem*, 2013, **14**, 1670–1675; T. Tsuchiya, T. Wakahara, S. Shirakura, Y. Maeda, T. Akasaka, K. Kobayashi, S. Nagase, T. Kato and K. M. Kadish, *Chem. Mater.*, 2004, **16**, 4343–4346.
4 P. Jakes and K. P. Dinse, *J. Am. Chem. Soc.*, 2001, **123**, 8854–8855.
5 A. A. Popov, A. D. Pykhova, I. N. Ioffe, F.-F. Li and L. Echegoyen, *J. Am. Chem. Soc.*, 2014, **136**, 13436–13441; B. Elliott, A. D. Pykhova, J. Rivera, C. M. Cardona, L. Dunsch, A. A. Popov and L. Echegoyen, *J. Phys. Chem. C*, 2013, **117**, 2344–2348; A. A. Popov, N. B. Shustova, A. L. Svitova, M. A. Mackey, C. E. Coumbe, J. P. Phillips, S. Stevenson, S. H. Strauss, O. V. Boltalina and L. Dunsch, *Chem. – Eur. J.*, 2010, **16**, 4721–4724.
6 D. V. Konarev, S. S. Khasanov, A. Otsuka, M. Maesato, G. Saito and R. N. Lyubovskaya, *Angew. Chem., Int. Ed.*, 2010, **49**, 4829–4832.
7 D. V. Konarev and R. N. Lyubovskaya, *Russ. Chem. Rev.*, 2012, **81**, 336–366.
8 C. M. Cardona, B. Elliott and L. Echegoyen, *J. Am. Chem. Soc.*, 2006, **128**, 6480–6485; S. F. Yang, M. Zalibera, P. Rapta and L. Dunsch, *Chem. – Eur. J.*, 2006, **12**, 7848–7855.
9 B. Elliott, L. Yu and L. Echegoyen, *J. Am. Chem. Soc.*, 2005, **127**, 10885–10888.
10 P. Rapta, A. A. Popov, S. F. Yang and L. Dunsch, *J. Phys. Chem. A*, 2008, **112**, 5858–5865.
11 A. A. Popov, S. M. Avdoshenko, G. Cuniberti and L. Dunsch, *J. Phys. Chem. Lett.*, 2011, 1592–1600.
12 D. V. Konarev, S. S. Khasanov, G. Saito, A. Otsuka, Y. Yoshida and R. N. Lyubovskaya, *J. Am. Chem. Soc.*, 2003, **125**, 10074–10083.
13 H. Ueno, S. Aoyagi, Y. Yamazaki, K. Ohkubo, N. Ikuma, H. Okada, T. Kato, Y. Matsuo, S. Fukuzumi and K. Kokubo, *Chem. Sci.*, 2016, DOI: 10.1039/C6SC01209D.
14 L. Feng, T. Tsuchiya, T. Wakahara, T. Nakahodo, Q. Piao, Y. Maeda, T. Akasaka, T. Kato, K. Yoza, E. Horn, N. Mizorogi and S. Nagase, *J. Am. Chem. Soc.*, 2006, **128**, 5990–5991.
15 M. Yamada, H. Kurihara, M. Suzuki, M. Saito, Z. Slanina, F. Uhlik, T. Aizawa, T. Kato, M. M. Olmstead, A. L. Balch, Y. Maeda, S. Nagase, X. Lu and T. Akasaka, *J. Am. Chem. Soc.*, 2015, **137**, 232–238.
16 L. Bao, C. Pan, Z. Slanina, F. Uhlik, T. Akasaka and X. Lu, *Angew. Chem., Int. Ed.*, 2016, **55**, 9234–9238.
17 L. Bao, M. Chen, C. Pan, T. Yamaguchi, T. Kato, M. M. Olmstead, A. L. Balch, T. Akasaka and X. Lu, *Angew. Chem., Int. Ed.*, 2016, **55**, 4242–4246.
18 M. Chen, L. Bao, M. Ai, W. Shen and X. Lu, *Chem. Sci.*, 2016, **7**, 2331–2334.
19 S. Wang, J. Huang, C. Gao, F. Jin, Q. Li, S. Xie and S. Yang, *Chem. – Eur. J.*, 2016, **22**, 8309–8315.
20 S. Stevenson, G. Rice, T. Glass, K. Harich, F. Cromer, M. R. Jordan, J. Craft, E. Hadju, R. Bible, M. M. Olmstead, K. Maitra, A. J. Fisher, A. L. Balch and H. C. Dorn, *Nature*, 1999, **401**, 55–57.
21 A. A. Popov and L. Dunsch, *J. Am. Chem. Soc.*, 2008, **130**, 17726–17742.
22 M. Krause, H. Kuzmany, P. Georgi, L. Dunsch, K. Vietze and G. Seifert, *J. Chem. Phys.*, 2001, **115**, 6596–6605.
23 P. W. Stephens, G. Bortel, G. Faigel, M. Tegze, A. Janossy, S. Pekker, G. Oszlanyi and L. Forro, *Nature*, 1994, **370**, 636–639.

